MDPI

*Article*

# Corrosion Behavior of the AZ31 Mg Alloy in Neutral Aqueous Solutions Containing Various Anions

**Duyoung Kwon** [1,2] , **Hien Van Pham** [1,3], **Pungkeun Song** [2,*] **and Sungmo Moon** [1,2,*]

1 Nano-Surface Materials Division, Korea Institute of Materials Science, Changwon 51508, Republic of Korea; legel@kims.re.kr (D.K.); phamvanhien@kims.re.kr (H.V.P.)
2 Department of Materials Science and Engineering, Pusan National University, Busan 46241, Republic of Korea
3 Advanced Materials Engineering, University of Science and Technology, Daejeon 34113, Republic of Korea
* Correspondence: pungkeun@pusan.ac.kr (P.S.); sungmo@kims.re.kr (S.M.)

**Abstract:** This work demonstrates the corrosion behavior of the AZ31 Mg alloy as a function of an immersion time of 48 h in 0.1 M HCl, $H_2SO_4$, $H_3PO_4$ and HF solutions, in which pH was adjusted to 6 to exclude the contribution of hydrogen ions ($H^+$) and hydroxide ions ($OH^-$). In situ observations, open circuit potential (OCP), weight changes and AC impedance measurements were performed with an immersion time of 48 h and the morphologies and chemical compositions of the surface products after 48 h of immersion were analyzed by SEM, EDS and XPS. In the chloride ion ($Cl^-$)-containing solution, the corrosion of the AZ31 Mg alloy initiated locally and propagated discontinuously over the surface with immersion time. The OCP value of the AZ31 Mg alloy showed an initial increase from $-1.51\ V_{Ag/AgCl}$ to $-1.47\ V_{Ag/AgCl}$ after about 5 h of immersion and then a decrease to $-1.51\ V_{Ag/AgCl}$ due to corrosion initiation. In the $F^-$-containing solution, after 48 h of immersion, the OCP showed an extremely large value of $-0.6\ V_{Ag/AgCl}$, while the relatively lower values of $-1.52\ V_{Ag/AgCl}$, $-1.59\ V_{Ag/AgCl}$ were seen in the solutions containing $SO_4^{2-}$ and $PO_4^3$, respectively. In the sulfate ion ($SO_4^{2-}$)-containing neutral aqueous solution, needle-like surface films were formed and there were no changes in the weight of the AZ31 Mg alloy with immersion time. In the phosphate ion ($PO_4^{3-}$)-containing neutral aqueous solution, a vigorous gas evolution occurred, together with the formation of black surface films with cracks, and a high corrosion rate of $-13.8018 \times 10^{-3}\ g \cdot cm^{-2} \cdot day^{-1}$ was obtained. In the fluoride ion ($F^-$)-containing neutral aqueous solution, a surface film with crystalline grains of $MgF_2$ was formed and the weight of the AZ31 Mg alloy increased continuously with immersion time. In conclusion, the corrosion of the AZ31 Mg alloy occurred uniformly in neutral phosphate solution but locally in chloride solution. No corrosion was observed in either the neutral sulfate or fluoride solutions.

**Keywords:** AZ31 Mg alloy; anions; corrosion; neutral aqueous solution; weight change

## 1. Introduction

The AZ31 Mg alloy is commonly used for a wide range of industrial applications due to its low density, high strength-to-weight ratio, good electromagnetic shielding, high vibration absorption property, exceptional castability and recyclability [1–4]. Mg is the most active metal among structural metallic materials due to the high chemical activity of magnesium ($E^o = -2.536$ V vs. NHE at 25 °C). The AZ31 Mg alloy contains 3% Al and 1% Zn. The alloying elements of Al and Zn can improve mechanical properties, formability and creep resistance, making alloys suitable for various industrial applications. However, these alloying elements can not only accelerate corrosion via a galvanic coupling effect but also by forming defects in surface films that are formed naturally [5–9]. Thus, Mg alloys can become quite susceptible to corrosion in atmospheric environments. The corrosion problem of Mg alloys has limited their industrial applications.

The corrosion behavior of magnesium alloys is affected by various factors, including the composition of the materials and environments [10–16]. When Mg alloys are exposed

to aqueous environments, various anions present in the aqueous environments can lead to the formation of surface films with various thicknesses, morphologies and chemical compositions. The corrosion resistance of Mg alloys is dependent on the nature of the surface films that are formed spontaneously. Chloride ions ($Cl^-$) are typical anions in atmospheric environments [17–19]. They play a significant role in promoting the corrosion of Mg alloys due to their aggressive nature in penetrating and disrupting the native oxide films that are formed on Mg alloy surfaces.

Sulfate ions ($SO_4^{2-}$) can also have a significant impact on the corrosion behavior of Mg alloys. When Mg alloys come into contact with water containing $SO_4^{2-}$ ions, soluble magnesium sulfate ($MgSO_4$) can be formed as a reaction product on the Mg alloy surfaces [20–22]. When $MgSO_4$ products are dissolved in water, the fresh metal surfaces are exposed to corrosive environments, leading to the corrosion of the Mg alloys. Phosphate ions ($PO_4^{3-}$) are known to improve the corrosion resistance of Mg alloys by forming chemical conversion coatings [23]. Fluoride ions ($F^-$) can improve the corrosion resistance of Mg alloys by forming stable surface films of $MgF_2$ [24–26]. However, since many works [23–26] have been conducted in acidic or alkaline solutions, the contributions of $H^+$ and $OH^-$ ions to the formation of surface films cannot be excluded. When a solution's pH is adjusted to neutral, the contributions of $H^+$ and $OH^-$ ions can become negligibly small.

In this work, in order to study the roles of four different anions ($Cl^-$, $SO_4^{2-}$, $PO_4^{3-}$ and $F^-$) in the formation of surface films and the corrosion of the AZ31 Mg alloy, we used neutral aqueous solutions with pH 6, which were prepared by adding small amounts of a 10 M NaOH solution into 0.1 M HCl, 0.1 M $H_2SO_4$, 0.1 M $H_3PO_4$ and 0.1 M HF solutions. The corrosion behavior of the AZ31 Mg alloy was investigated through open circuit potential (OCP) measurements, electrochemical impedance spectroscopy (EIS) and weight gain/loss measurements, while the morphological and chemical compositions of the surface films formed during immersion in the neutral aqueous solutions containing four different anions were analyzed using scanning electron microscopy (SEM), energy dispersive spectroscopy (EDS) and X-ray photoelectron spectroscopy (XPS).

## 2. Experiments

### 2.1. Sample Preparation

Commercial AZ31B Mg alloy plates (wt.%: Al = 2.94; Zn = 0.8; Mn = 0.3; Si < 0.1; Fe < 0.005; Cu < 0.05; Mg balance) were used for the current work. One side of each plate was polished using 220 grit to 4000 grit SiC papers with 98% ethyl alcohol and was then masked to expose an area of 1.3 $cm^2$ using polyester tape. A copper wire was connected to the backside of each plate to form a direct electrical connection to a potentiostat/galvanostat. The contact resistance between the Cu wires and the plates was maintained at less than 0.5 m$\Omega$.

### 2.2. Immersion Tests and Electrochemical Measurements

The immersion tests of the AZ31 Mg alloy specimens were performed over 48 h in 1 L of 0.1 M HCl, $H_2SO_4$, $H_3PO_4$ and HF solutions at 20 ± 0.5 °C. The solution pH was adjusted to 6 by adding small amounts of a 10 M NaOH solution. During the immersion tests, the surfaces of the AZ31 Mg alloys were photographed using a digital camera under the same illumination conditions and the open circuit potential (OCP) and electrochemical impedance spectroscopy (EIS) were measured with immersion time. The weights of the specimens (which were about 46 $cm^2$) were measured before and during immersion at 12, 24, 36 and 48 h at 20 ± 0.5 °C using a balance (METTLER TOLEDO, XPE205V, Columbus, OH, United States) and the weight changes were calculated by subtracting the weights before immersion from those during and after immersion.

The OCP and EIS measurements were conducted using an electrochemical workstation (Biologic VMP3 multichannel potentiostat, BioLogic, Seyssinet-Pariset, France) with a three-electrode system, including a working electrode, a counter electrode (Pt mesh) and a reference electrode (Ag/AgCl electrode). The EIS measurements were performed

in a frequency range from $10^5$ to $10^{-1}$ Hz, with a signal amplitude of 10 mV. The EIS results obtained were fitted by EC-Lab software using equivalent circuit models that were suggested in a previous paper [27]. The OCP and EIS measurements were repeated more than three times to check the experiment's reproducibility.

### 2.3. Characterization of Surface Morphologies and Chemical Compositions

The surface morphologies of the AZ31 Mg alloys that had been immersed for 48 h in neutral aqueous solutions containing different anions were observed using a scanning electron microscope (SEM, JSM-6610LV, JEOL Ltd., Tokyo, Japan) and field emission scanning electron microscopy (FE-SEM, JEOL JSM-7900F, JEOL Ltd., Tokyo, Japan). The chemical compositions of the surface films were analyzed using an X-ray energy dispersive spectrometer (EDS, Oxford X-Max, Oxford Instruments NanoAnalysis, High Wycombe, UK) and X-ray photoelectron spectroscopy (XPS, Kratos AXIS supra$^+$, Kratos Analytical Ltd., Manchester, UK). XPS survey scans and detailed scans of the Mg 1s, Cl 2p, S 2p, P 2p and F 2p photoelectron emissions were conducted for each sample. The binding energies of all XPS spectra were referenced to the C 1s peak at 284.6 eV.

## 3. Results and Discussion

### 3.1. In Situ Observations of the AZ31 Mg Alloy Surfaces during Immersion

Figure 1 presents the changes in surface color and gas evolution with immersion time of the AZ31 Mg alloy surfaces in the neutral aqueous solutions containing different anions ($Cl^-$, $SO_4^{2-}$, $PO_4^{3-}$ and $F^-$). In the solutions containing $Cl^-$, $SO_4^{2-}$ and $F^-$, several gas bubbles were partly formed during immersion. The bubbles became larger with immersion time and were then removed from the AZ31 Mg alloy surfaces after several hours of immersion. Gas evolution occurred vigorously from the moment of immersion in the $PO_4^{3-}$-containing solution and its rate lowered with immersion time. No further gas generation was observed after 1 h of immersion. Considering that the gas bubbles were hydrogen gas formed at cathodic sites, such as second-phase particles or impurities, by local cell reactions, it seemed reasonable to conclude that the corrosion of the AZ31 Mg alloy occurred rapidly during the initial stages of immersion in the $PO_4^{3-}$-containing solution but was relatively slow in the $Cl^-$-, $SO_4^{2-}$- and $F^-$-containing solutions.
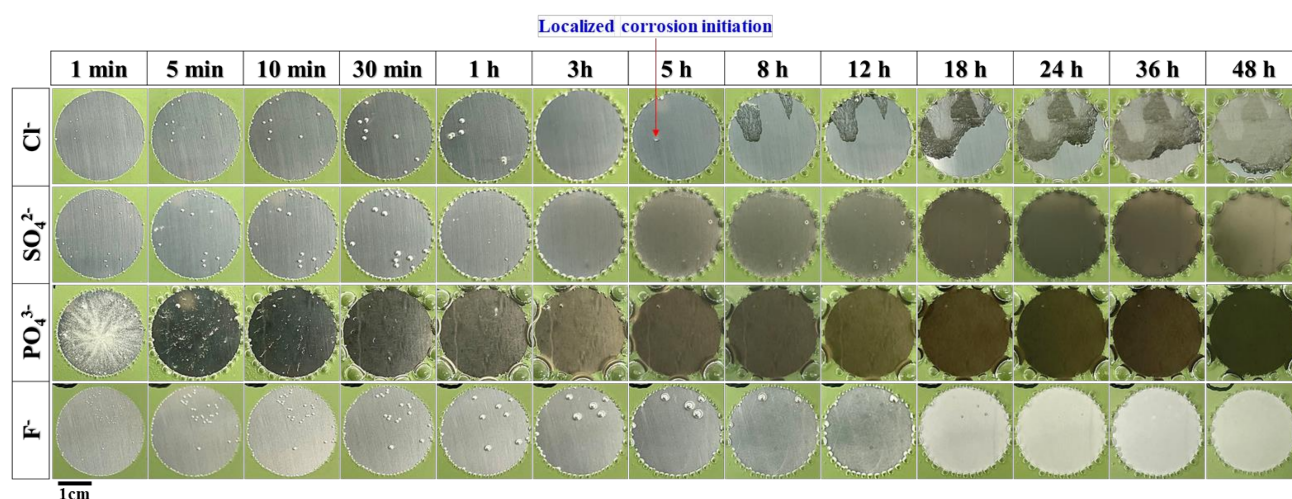


**Figure 1.** Photographs of the AZ31 Mg alloy surfaces during immersion for 48 h in 0.1 M HCl, $H_2SO_4$, $H_3PO_4$ and HF solutions at $20 \pm 0.5\ °C$. The solution pH was adjusted to 6 by adding 10 M NaOH solution.

Changes in the color of the AZ31 Mg alloy surfaces with immersion time were crucially dependent on the type of anion present in the neutral aqueous solution. In the $SO_4^{2-}$-and $PO_4^{3-}$-containing solutions, the color of the AZ31 Mg alloy surfaces became darker with

immersion time, while they became brighter after immersion for 18 h in the $F^-$-containing neutral solution. The darkened surfaces with immersion time could have been due to the reduced reflection of light resulting from the formation of more porous surface films. In contrast, the brightened surfaces with immersion time indicated the formation of denser surface films that could reflect light more efficiently.

It was noticed that the surface color of the AZ31 Mg alloy specimens became significantly darker even after short periods of immersion (5 min) in the $PO_4^{3-}$-containing solution. The darkened surfaces seemed to originate from the highly porous structures of the surface films, as revealed in a previous paper [27]. By contrast, the surface color of the AZ31 Mg alloy became largely brighter after 18 h of immersion in the $F^-$-containing solution, implying that dense surface films were formed after long periods of immersion. In the solution containing $SO_4^{2-}$, the surface color changed after 3 h of immersion and gradually became darker with immersion time up to 24 h.

The excessive gas evolution on the AZ31 Mg alloy surfaces during the initial stages of immersion in the $PO_4^{3-}$-containing solution was thought to be caused by the fast dissolution of the Mg alloy. The fast dissolution of the AZ31 Mg alloy was assumed to occur due to the formation of extremely porous complex films, as readily inferred from the dark surface colors after 5 min of immersion (Figure 1).

In the $Cl^-$-containing solution, corrosion was initiated after 5 h of immersion at the point indicated by the red arrow in Figure 1 and the corroded area expanded with immersion time. It was noted that the corrosion of the AZ31 Mg alloy appeared to be localized between 5 h and 36 h of immersion but occurred over almost the entire surfaces of the AZ31 Mg alloy specimens after 48 h of immersion.

### 3.2. Open Circuit Potential Transients

Figure 2 presents the changes in the open circuit potential (OCP) value of the AZ31 Mg alloy with time up to 48 h when immersed in neutral aqueous solutions containing $Cl^-$, $SO_4^{2-}$, $PO_4^{3-}$ and $F^-$ ions. The OCP value showed an extremely large increase from about $-1.5$ $V_{Ag/AgCl}$ to $-0.6$ $V_{Ag/AgCl}$ in the $F^-$-containing neutral solution. In general, the OCP value has the tendency to corrode or passivate metallic materials, resulting from electrochemical reactions with surrounding electrolytes. Thus, it could be said that the large increase in OCP up to about 18 h of immersion in the $F^-$-containing solution was due to continuous electrochemical reactions occurring throughout the porous surface films. The porous films seemed to be transformed into denser films with immersion time up to 18 h.
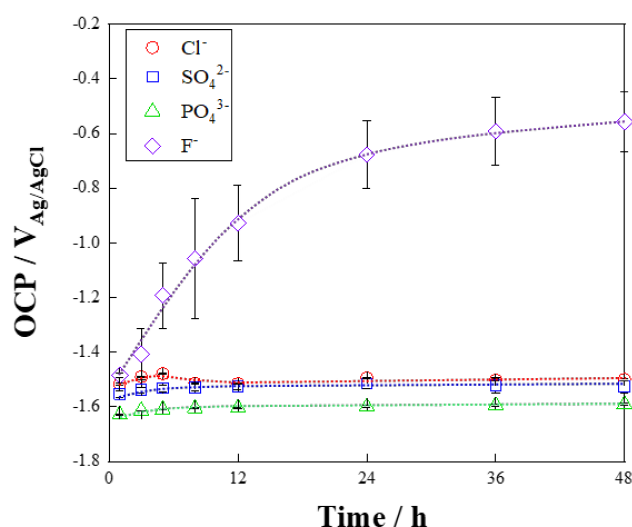


**Figure 2.** The OCP of the AZ31 Mg alloy specimens during immersion for 48 h in 0.1 M HCl, $H_2SO_4$, $H_3PO_4$ and HF solutions at $20 \pm 0.5$ °C. The solution pH was adjusted to 6 by adding 10 M NaOH solution.

In the $Cl^-$ containing solution, the OCP value showed an initial increase from $-1.51 V_{Ag/AgCl}$ to $-1.47 V_{Ag/AgCl}$ with immersion time up to about 5 h (Figure 2) but it decreased after 5 h to $-1.51 V_{Ag/AgCl}$, which was related with the initiation of corrosion, as can be seen in Figure 1. In the solutions containing $SO_4^{2-}$ and $PO_4^{3-}$, the open circuit potential slightly increased from $-1.55 V_{Ag/AgCl}$ to $-1.52 V_{Ag/AgCl}$ and from $-1.62 V_{Ag/AgCl}$ to $-1.59 V_{Ag/AgCl}$, respectively, for the first 8 h of immersion and then reached a stable value (Figure 1). It should be pointed out that the OCP values showed negligibly small changes in the solutions containing $Cl^-$, $SO_4^{2-}$ and $PO_4^{3-}$ but large changes were observed in the $F^-$-containing neutral aqueous solution, depending on the specimen. The largely changeable OCP value of the specimens in the $F^-$-containing solution could have been caused by different electrochemical reactions on the Mg and the alloying elements of Al and Zn.

### 3.3. Weight Changes with Immersion Time

The weights of the AZ31 Mg alloy specimens were measured after immersion for 12, 24, 36 and 48 h in neutral aqueous solutions containing four different anions ($Cl^-$, $SO_4^{2-}$, $PO_4^{3-}$ and $F^-$) and the weight changes were calculated by subtracting the weights before immersion from those during and after immersion in the solutions. The weight changes are plotted in Figure 3 against immersion time. It was interesting to note that the weights of the AZ31 Mg alloy specimens increased with immersion time in the $Cl^-$- and $F^-$-containing neutral solutions. The increased weights revealed that more corrosion products or surface films formed than dissolved on the AZ31 Mg alloy surfaces. The corrosion products and surface film formed on AZ31 Mg alloys could have been $MgCl_2$ and $MgF_2$ in the $Cl^-$- and $F^-$-containing solutions, respectively.
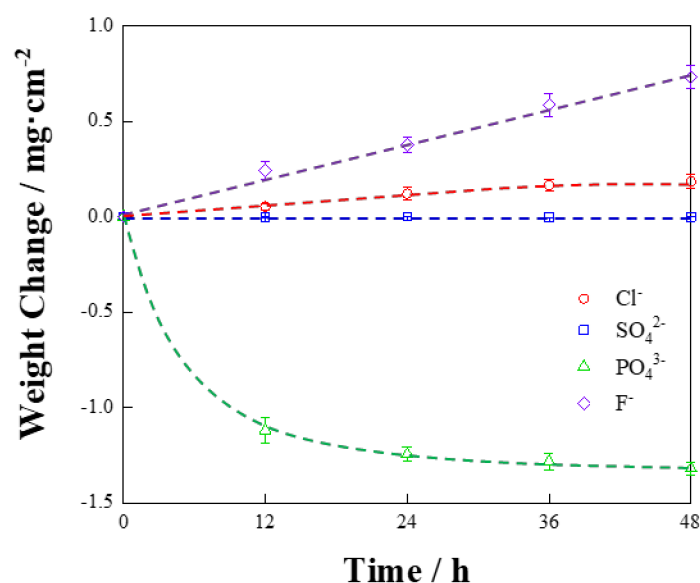


**Figure 3.** Changes in weight of the AZ31 Mg alloy specimens with immersion time in 0.1 M HCl, $H_2SO_4$, $H_3PO_4$ and HF solutions at $20 \pm 0.5\,°C$. The solution pH was adjusted to 6 by adding 10 M NaOH solution.

It was noticed that the increase in weight during immersion in the $Cl^-$-containing solution slowed down after 36 h, as shown in Figure 3 suggesting that the formation rate of the corrosion product $MgCl_2$ was higher than the dissolution rate of the AZ31 Mg alloy up to 36 h. On the other hand, the increase in weight during immersion in the $F^-$-containing solution did not slow down up to 48 h. This suggested that the $MgF_2$ film was sufficiently porous to grow continuously with immersion time in the $F^-$-containing neutral solution.

By contrast, the weight decreased with immersion time in the $PO_4^{3-}$-containing neutral solution. The weight decreased largely in the initial stages of immersion but slowed

with immersion time. These results indicated that the corrosion of the AZ31 Mg alloy by phosphate ions occurred largely in the initial stages of immersion and that the corrosion rate lowered with immersion time. Gas evolution was fast in the initial stages of immersion in the $PO_4^{3-}$-containing solution, shown in Figure 1, which was in good accordance with the large decrease in weight, as shown in Figure 3. The fast dissolution of the AZ31 Mg alloy in the initial stages of immersion revealed that black surface films were not as protective against corrosion. However, the lower weight reduction rate after 24 h of immersion in the $PO_4^{3-}$-containing solution suggested that the black surface films formed after more than 24 h were more protective against corrosion than those formed in the initial stages of immersion.

Surprisingly, no noticeable changes were detected in the weights of the AZ31 Mg alloy specimens in the $SO_4^{2-}$-containing neutral solution with immersion time up to 48 h. Considering that the slightly darker surface of the AZ31 Mg alloy after immersion for 36 h in the $SO_4^{2-}$-containing neutral solution (Figure 1) revealed the growth of complex surface films, probably magnesium sulfate films together with magnesium hydroxide films, the lack of changes in weight during immersion could suggest the excellent protective property of magnesium sulfate films against corrosion. The corrosion protective property of magnesium sulfate films will be discussed in detail in a subsequent paper.

The corrosion rate (CR, $g \cdot cm^{-2} \cdot day^{-1}$) of the AZ31 Mg alloy in the neutral aqueous solutions containing four different anions was calculated from the weight change data after 48 h of immersion. As a result, the corrosion rates in the neutral solutions containing $Cl^-$ ions, $SO_4^{2-}$ ions, $PO_4^{3-}$ ions and $F^-$ ions were found to be $1.9222 \times 10^{-3}$ $g \cdot cm^{-2} \cdot day^{-1}$, $-0.0023 \times 10^{-3}$ $g \cdot cm^{-2} \cdot day^{-1}$, $-13.8018 \times 10^{-3}$ $g \cdot cm^{-2} \cdot day^{-1}$ and $7.6280 \times 10^{-3}$ $g \cdot cm^{-2} \cdot day^{-1}$, respectively. Previous studies [28,29] have reported that the corrosion rate of the AZ31 Mg alloy in $Cl^-$ ion-containing solutions ranges from 0.02 to 7.2 mm/year, which equates to $0.009 \times 10^{-3}$ to $3.429 \times 10^{-3}$ $g \cdot cm^{-2} \cdot day^{-1}$. In this study, weight gain instead of weight loss was obtained during the initial stages of immersion up to 36 h in the neutral aqueous solution containing chloride ions. This was attributed to the formation of chloride films during the initial stages of immersion. Since the calculated corrosion rates in this study were based on data obtained from up to 48 h of immersion time, they did not reflect the long-term corrosion behavior of the AZ31 alloy. Thus, further research with longer exposure times is necessary for understanding the corrosion behavior over extended periods.

### 3.4. Electrochemical Impedance Spectroscopy

Figure 4 presents the Nyquist plots obtained from the AZ31 Mg alloy specimens with immersion time up to 48 h in neutral aqueous solutions containing various anions. In the solution containing $Cl^-$, two capacitance loops were identified in high-to-medium- and low-frequency regions up to 5 h of immersion, after which one capacitive loop and one inductive loop appeared. The diameter of the capacitance loop in the high-to-medium-frequency region increased with immersion time up to 5 h but largely decreased after 8 h.

In the solutions containing $SO_4^{2-}$ and $PO_4^{3-}$ ions, two capacitance loops were observed. The diameters of the high-frequency capacitance loops showed significant increases with immersion time. However, the diameters of the low-frequency capacitive loops showed slight decreases with immersion time in the solution containing $SO_4^{2-}$, while they increased slightly with immersion time in the solution containing $PO_4^{3-}$.

In the solution containing $F^-$, two capacitance loops were observed after the first 3 h of immersion and then only one large capacitance loop appeared. It was noted that the diameter of the high-frequency capacitance loop increased largely with immersion time in the $F^-$-containing solution compared to those in the $SO_4^{2-}$- and $PO_4^{3-}$-containing neutral aqueous solutions.
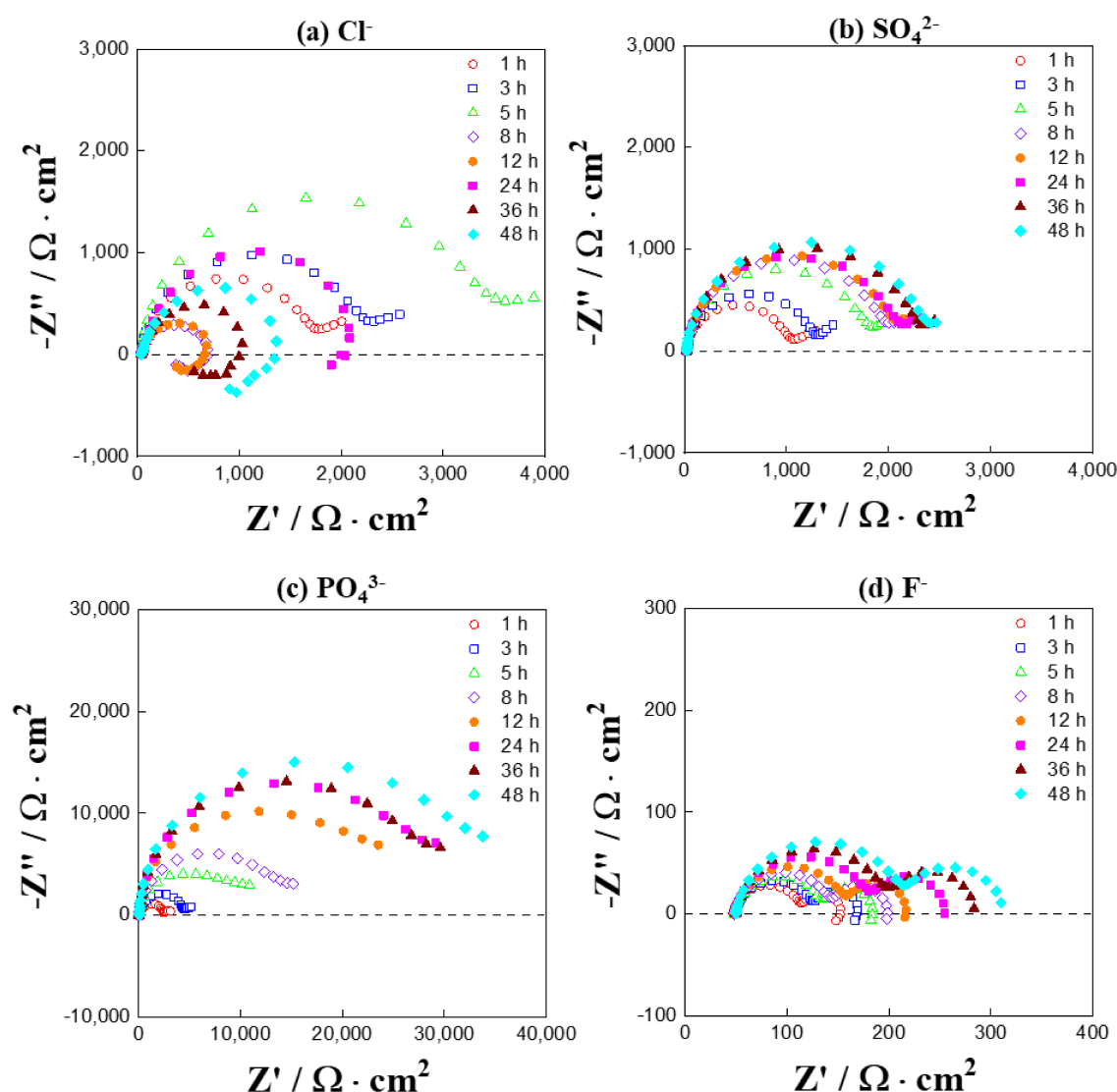
**Figure 4.** Nyquist plots obtained during the immersion of the AZ31 Mg alloy in (**a**) 0.1 M HCl, (**b**) $H_2SO_4$, (**c**) $H_3PO_4$ and (**d**) HF solutions at $20 \pm 0.5$ °C. The solution pH was adjusted to 6 by adding 10 M NaOH solution.

The EIS data in Figure 4 were fitted using equivalent circuit models that were suggested in a previous paper [21] and the resistance of the surface films is exhibited in Figure 5 as a function of immersion time. The film resistance increased with time in the initial stages of immersion in all the solutions up to 5 h and showed different values depending on the type of anion in the order of $F^- > Cl^- > SO_4^{2-} > PO_4^{3-}$, which was exactly the same order as the OCP values in Figure 2.

The film resistance decreased suddenly after 5 h of immersion in the $Cl^-$-containing solution, which was ascribed to the occurrence of corrosion, as depicted in Figure 1. The film resistance in the $Cl^-$-containing solution occasionally showed an increased value, as can be seen at 24 h of immersion in Figure 5. The increased film resistance at 24 h seemed to be related to the change in the color of the corroded region from black to white in Figure 1. The change in the color of the corroded region from black to white could indicate passivation by corrosion products. Further corrosion after 36 h of immersion in the $Cl^-$-containing solution resulted in a decrease in film resistance to the very low value of about 300 ohm $cm^{-2}$. It was noticeable that film resistance was largely changeable in the chloride ion-containing solution after the initiation of corrosion, which could have arisen from the formation and dissolution of corrosion products.
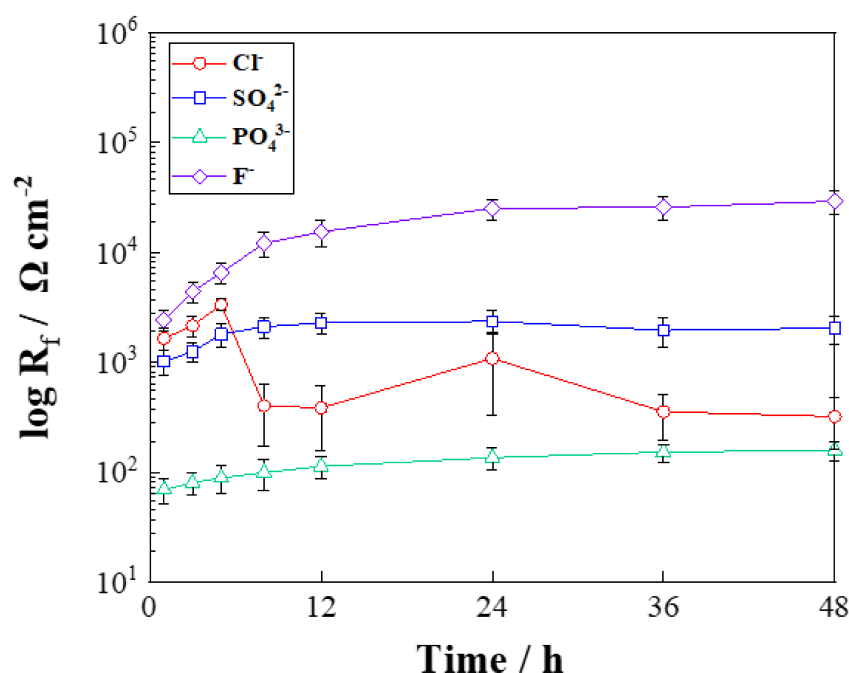
**Figure 5.** Plot of the surface film resistance of the AZ31 Mg alloy specimens (Figure 3) with immersion time.

*3.5. Morphologies and Compositions of the Surface Films*

Figure 6 shows the SEM images and EDS results of the AZ31 Mg alloy surfaces after immersion for 48 h in neutral aqueous solutions containing various anions. In the $Cl^-$-containing solution, the AZ31 Mg alloy surface partly corroded and porous corrosion products with cracks were observed at the corroded region. The porous corrosion products were found to contain mainly oxygen and magnesium, which could have been magnesium oxides or magnesium hydroxides. The very low chloride content of 0.56 at.% was observed in the porous corrosion products. Small pits and numerous scratches were also observed in the regions where corrosion was relatively less progressed (Figure 6f). The scratches disappeared after 48 h of immersion in the $SO_4^{2-}$, $PO_4^{3-}$ and $F^-$ ion-containing solutions, suggesting that dissolution and surface film formation reactions occurred significantly on the AZ31 Mg alloy surfaces.

In the solution containing $SO_4^{2-}$ ions, surface films with needle-like structures and cracks were formed over the entire surface of the AZ31 Mg alloy. The surface films contained about 38 at.% oxygen and a small amount of sulfur (Figure 6p), indicating that they consisted of mainly magnesium oxide/hydroxide and a small amount of magnesium sulfate ($MgSO_4$). It should be mentioned that the surface films consisting of magnesium oxide/hydroxide and a small amount of magnesium sulfate ($MgSO_4$) were very protective against further electrochemical reactions, so no changes in the weight of the AZ31 Mg alloy specimen were observed, as shown in Figure 3.

In the solution containing $PO_4^{3-}$, dark films were formed, as shown in Figure 1, and were easily detached by an air stream during drying after washing the specimens. The dark films were relatively thick and cracked into small pieces of about 100 microns in size. The dark films contained large amounts of oxygen (about 66 at.%) and phosphor (16.06 at.%) (Figure 6p). It was interesting to notice that the Al and Mg contents of the dark films were 7.28 at.% and 10.62 at.%, respectively, which were much higher than the original Al content of 3 wt.% and much lower than the original Mg content of about 96 wt.% in the AZ31 Mg alloy substrate. These results revealed that Al was not dissolved and remained by forming aluminum phosphate but Mg was dissolved easily during immersion in the $PO_4^{3-}$-containing neutral solution.
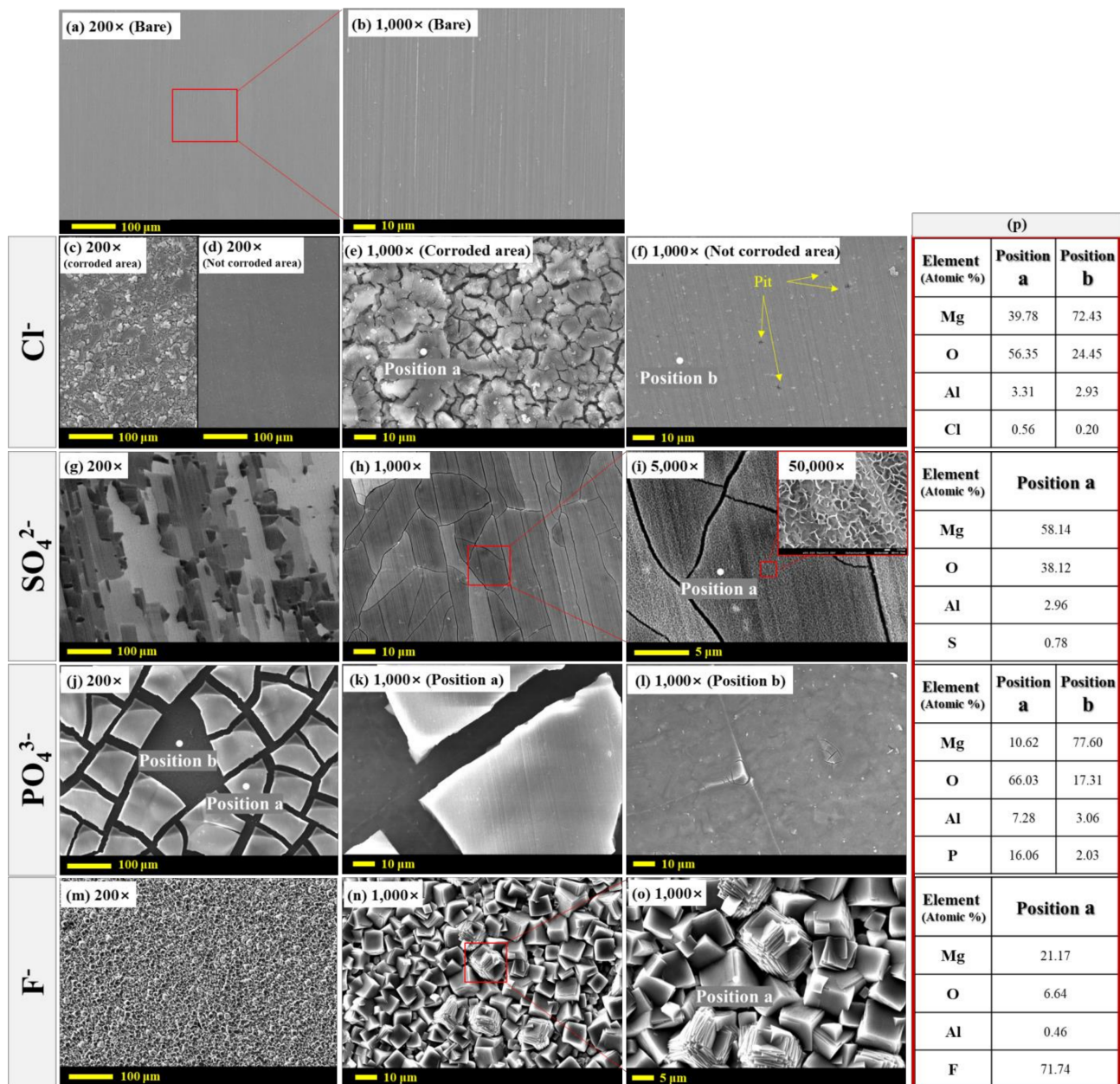
**Figure 6.** SEM images (**a–o**) and EDS results (**p**) of the AZ31 Mg alloy surfaces before (**a,b**) and after immersion for 48 h in 0.1 M HCl (**c–f**), $H_2SO_4$ (**g–i**), $H_3PO_4$ (**j–l**) and HF (**m–o**) solutions, in which pH was adjusted to 6 by adding 10 M NaOH solution.

The area from which the dark films were detached by the air stream during drying showed a very smooth and glossy surface and about 2 at.% phosphor was detected on the smooth surface. The small amount of P on the underlying smooth surface could be attributed to the presence of a very thin surface layer of $AlPO_4$ and $Mg_3(PO_4)_2$, through which electron beams could easily penetrate into the AZ31 substrate.

In the solution containing $F^-$, a number of small rectangular grains formed densely on the AZ31 Mg alloy surface. The crystalline grains consisted of about 21 at.% magnesium, 6.64 at.% oxygen and about 72% fluorine (Figure 6p). The extremely high content of fluorine and the low contents of oxygen and magnesium reflected the fact that the coatings with rectangular grains that formed in the neutral fluoride solution were mainly composed of magnesium fluoride ($MgF_2$) and that the content of magnesium oxide/hydroxide was very low. $MgF_2$ is a highly an ionic compound with a strong ionic bond between the magnesium

cation ($Mg^{2+}$) and the fluoride anion ($F^−$). This ionic bond results in a strong crystal lattice structure with high thermal and chemical stability. However, the large increases in weight and open circuit potential with immersion time suggested that the $MgF_2$ films were not physically dense and that the diffusion of $F^−$ ions and $Mg^{2+}$ ions through the fluoride films was easy. It was also interesting that the Al content in the coatings formed in the neutral fluoride solution lowered to 0.46 at.%, indicating the dissolution of Al by fluoride ions.

In order to further identify the chemical states of the surface products formed on the AZ31 Mg alloy surfaces after immersion for 48 h in neutral aqueous solutions containing various anions, the surface films were analyzed by XPS and the deconvolved XPS spectra are exhibited in Figure 6. In the $Cl^−$ ion-containing solution, the Mg 1s spectrum was fitted into three peaks at 1302.7 eV, 1303.8 eV and 1304.6 eV, which corresponded to $Mg(OH)_2$, MgO and $MgCl_2$, respectively. The peak intensities appeared to decrease in the order of $MgO > Mg(OH)_2 > MgCl_2$, suggesting that the corrosion products formed in the neutral chloride solution were composed of a large amount of magnesium oxide and magnesium hydroxide, together with a small amount of magnesium chloride ($MgCl_2$). The Cl 2p spectrum was fitted into two peaks at 197.9 eV and 199.6 eV, which corresponded to chemisorbed chloride ions and $MgCl_2$, respectively.

In the $SO_4^{2−}$ ion-containing solution, the Mg 1s spectrum peaked at 1302.7 eV, 1303.8 eV and 1305 eV, which corresponded to $Mg(OH)_2$, MgO and $MgSO_4$, respectively. The peak intensities revealed that the flake-like surface films in Figure 6a consisted of mainly $Mg(OH)_2$ and a small amount of MgO and $MgSO_4$. This was in good agreement with the results obtained by EDS analysis in Figure 6b. The S 2p spectrum at 168.5 eV corresponded to chemisorbed sulfate ions.

In the $PO_4^{3−}$ ion-containing solution, the Mg 1s spectrum showed three peaks at 1302.7 eV, 1303.8 eV and 1304.1 eV, which corresponded to $Mg(OH)_2$, MgO and $Mg_3(PO_4)_2$, respectively. The peak intensity of the passive films containing magnesium phosphate ($Mg_3(PO_4)_2$) was relatively lower than that of MgO (Figure 7c). Thus, it could be said that the surface films consisting of a large amount of MgO and a small amount of $Mg_3(PO_4)_2$ did not effectively protect the AZ31 Mg alloy surfaces, as indicated by the high weight loss in Figure 3c. The P 2p spectrum peaked at 133.4~134.3 eV, corresponding to phosphorus groups (P-O and P=O).

In the $F^−$ ion-containing solution, two peaks at 1303.8 eV and 1304.8 eV, corresponding to MgO and $MgF_2$, respectively, were obtained (Figure 7d). The $MgF_2$ peak was clearly observed and its intensity was higher than that of MgO, indicating that the $F^−$ ions formed very stable films of $MgF_2$ together with MgO on the AZ31 Mg alloy surfaces. It should be mentioned that $Mg(OH)_2$ was not present in the surface films formed in the $F^−$ ion-containing neutral aqueous solution.
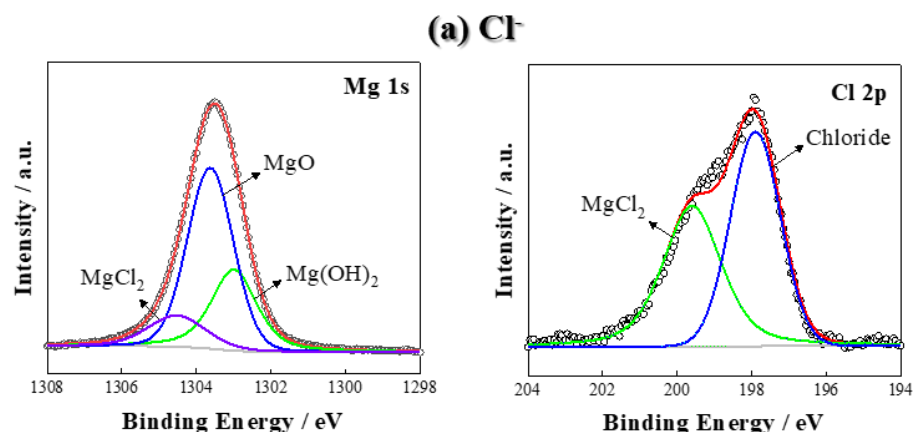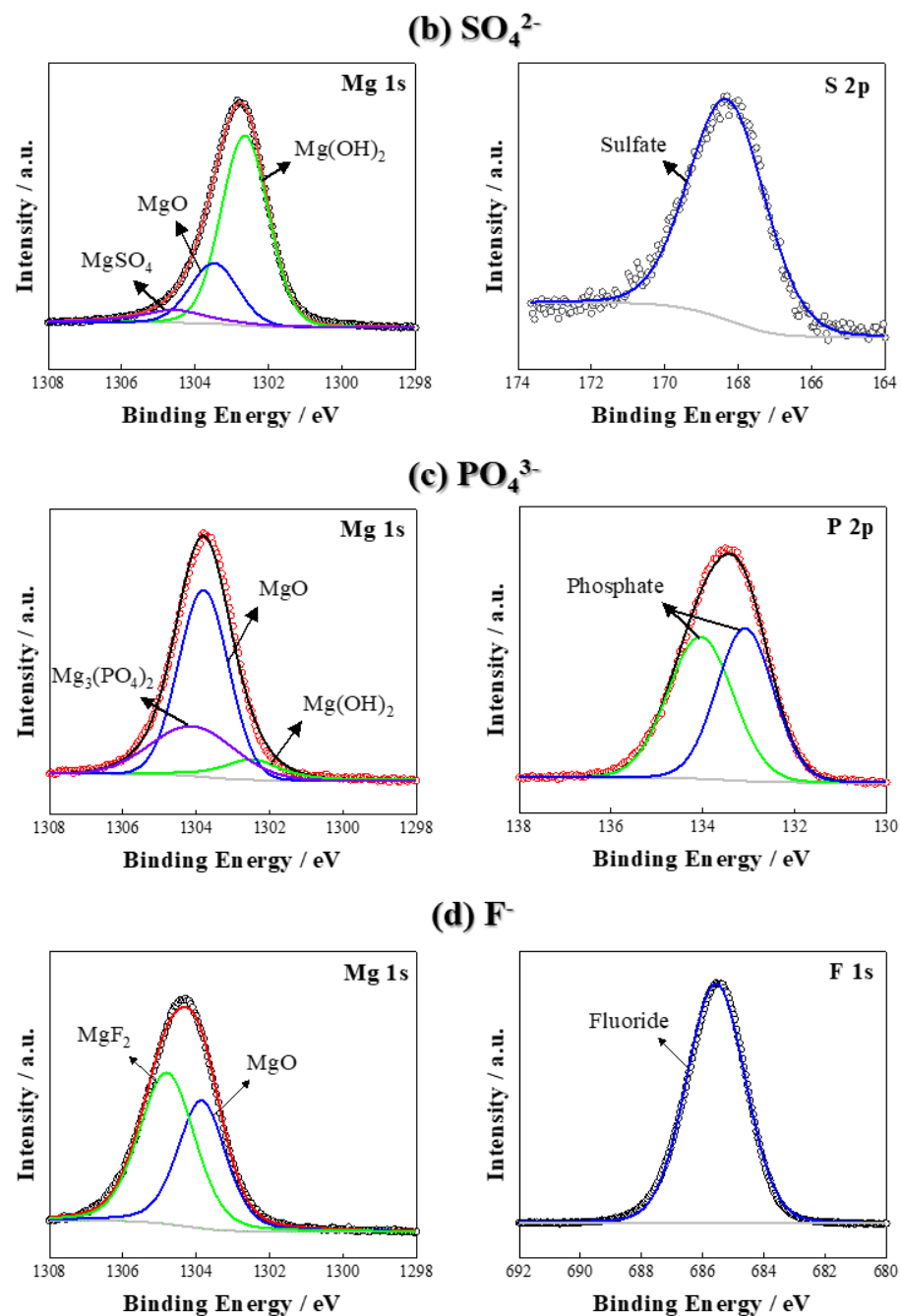


**Figure 7.** *Cont.*

**(b) SO$_4$$^{2-}$**



**(c) PO$_4$$^{3-}$**



**(d) F$^-$**



**Figure 7.** XPS spectra of the AZ31 Mg alloy specimens after immersion for 48 h in (**a**) 0.1 M HCl, (**b**) H$_2$SO$_4$, (**c**) H$_3$PO$_4$ and (**d**) HF solutions, in which pH was adjusted to 6 by adding 10 M NaOH solution.

## 4. Conclusions

In this work, the corrosion behavior of the AZ31 Mg alloy was examined in neutral aqueous solutions containing various anions (Cl$^-$, SO$_4$$^{2-}$, PO$_4$$^{3-}$ and F$^-$). The corrosion of the AZ31 Mg alloy appeared to largely depend on the type of anion present in the neutral aqueous solution. When the AZ31 Mg alloy was immersed in a Cl$^-$-containing solution, the corrosion of the AZ31 Mg alloy occurred locally initially and then the corroded area expanded discontinuously with immersion time. The open circuit potential value of the AZ31 Mg alloy in the Cl$^-$-containing neutral solution showed an initial increase from $-1.51$ V$_{Ag/AgCl}$ to $-1.47$ V$_{Ag/AgCl}$ with immersion time up to about 5 h and then a decrease after 5 h to $-1.51$ V$_{Ag/AgCl}$ due to corrosion initiation. In the F$^-$-containing solution, after 48 h of immersion, the OCP value showed an extremely large value of

$-0.6~V_{Ag/AgCl}$, while the relatively lower values of $-1.52~V_{Ag/AgCl}$ and $-1.59~V_{Ag/AgCl}$ were observed in the solutions containing $SO_4^{2-}$ and $PO_4^{3-}$, respectively. The weights of the specimens increased with immersion time in the $Cl^-$-containing solution up to 36 h by forming porous corrosion products containing $MgCl_2$, $MgO$ and $Mg(OH)_2$. In the solution containing $SO_4^{2-}$ ions, no weight changes were observed and slightly dark surface films with cracks were formed. In the $PO_4^{3-}$-containing neutral solution, vigorous gas evolution was observed in the initial stages of immersion and black surface films with cracks were formed, which contained about 66 at.% O, 16.06 at.% P, 7.28 at.% Al and 10.62 at.% Mg, revealing that Al was not dissolved and remained to form aluminum phosphate but Mg was dissolved easily in the $PO_4^{3-}$-containing neutral solution. The black surface films were easily peeled off from the surfaces using air streams and a large weight loss was observed in the initial stages of immersion in the $PO_4^{3-}$-containing neutral solution, showing a corrosion rate of $-13.8018 \times 10^{-3}~g \cdot cm^{-2} \cdot day^{-1}$. In the $F^-$ containing neutral solution, the weights of the specimens increased continuously with immersion time due to the formation of $MgF_2$ films with crystalline grains.

**Data Availability Statement:** Not applicable.

**Conflicts of Interest:** The authors declare that they have no conflict of interest.

## References

1. Mordike, B.L.; Ebert, T. Magnesium: Properties—applications—potential. *Mater. Sci. Eng. A-Struct. Mater. Prop. Microstruct.* **2001**, *302*, 37–45. [CrossRef]
2. Staiger, M.P.; Pietak, A.M.; Huadmai, J.; Dias, G. Magnesium and its alloys as orthopedic biomaterials: A review. *Biomaterials* **2006**, *27*, 1728–1734. [CrossRef] [PubMed]
3. Song, J.; She, J.; Chen, D.; Pan, F. Latest research advances on magnesium and magnesium alloys worldwide. *J. Magnes. Alloy.* **2020**, *8*, 1–41. [CrossRef]
4. Yang, Y.; Xiong, X.; Chen, J.; Peng, X.; Chen, D.; Pan, F. Research advances in magnesium and magnesium alloys worldwide in 2020. *J. Magnes. Alloy.* **2021**, *9*, 705–747. [CrossRef]
5. Atrens, A.; Winzer, N.; Dietzel, W. Stress corrosion cracking of magnesium alloys. *Adv. Eng. Mater.* **2011**, *13*, 11–18. [CrossRef]
6. Song, Y.; Han, E.-H.; Shan, D.; Yim, C.D.; You, B.S. The role of second phases in the corrosion behavior of Mg–5Zn alloy. *Corrosion Sci.* **2012**, *60*, 238–245. [CrossRef]
7. Feng, H.; Liu, S.; Du, Y.; Lei, T.; Zeng, R.; Yuan, T. Effect of the second phases on corrosion behavior of the Mg-Al-Zn alloys. *J. Alloy. Compd.* **2017**, *695*, 2330–2338. [CrossRef]
8. Shih, C.-H.; Huang, C.-Y.; Hsiao, T.-H.; Lin, C.-S. The effect of the secondary phases on the corrosion of AZ31B and WE43-T5 Mg alloys. *Corrosion Sci.* **2023**, *211*, 110920. [CrossRef]
9. Zhang, K.; Wang, C.; Liu, S.; Guan, K.; Li, M.-X.; Zhang, L.-Y.; Wang, H.-Y. New insights on corrosion behavior of aging precipitates in dilute Mg-Al-Ca alloy by experiments and first-principles calculations. *Corrosion Sci.* **2023**, 111254, *in press*. [CrossRef]
10. Song, G.L.; Atrens, A. Corrosion Mechanisms of Magnesium Alloys. *Adv. Eng. Mater.* **1999**, *1*, 11–33. [CrossRef]
11. Neil, W.; Forsyth, M.; Howlett, P.C.; Hutchinson, C.; Hinton, B.R.W. Corrosion of magnesium alloy ZE41–The role of microstructural features. *Corrosion Sci.* **2009**, *51*, 387–394. [CrossRef]
12. Liu, L.; Schlesinger, M. Corrosion of magnesium and its alloys. *Corrosion Sci.* **2009**, *51*, 1733–1737. [CrossRef]
13. Esmaily, M.; Svensson, J.E.; Fajardo, S.; Birbilis, N.; Frankel, G.S.; Virtanen, S.; Arrabal, R.; Thomas, S.; Johansson, L.G. Fundamentals and advances in magnesium alloy corrosion. *Prog. Mater. Sci.* **2017**, *89*, 92–193. [CrossRef]
14. Shahabi-Navid, M.; Cao, Y.; Svensson, J.-E.; Allanore, A.; Birbilis, N.; Johansson, L.-G.; Esmaily, M. On the early stages of localised atmospheric corrosion of magnesium–aluminium alloys. *Sci. Rep.* **2020**, *10*, 20972. [CrossRef]
15. Nachtsheim, J.; Burja, J.; Ma, S.; Markert, B. Long-Term in Vitro Corrosion of Biodegradable WE43 Magnesium Alloy in DMEM. *Metals* **2022**, *12*, 2062. [CrossRef]
16. Vinogradov, A.; Merson, E.; Myagkikh, P.; Linderov, M.; Brilevsky, A.; Merson, D. Attaining High Functional Performance in Biodegradable Mg-Alloys: An Overview of Challenges and Prospects for the Mg-Zn-Ca System. *Materials* **2023**, *16*, 1324. [CrossRef] [PubMed]

17. Ambat, R.; Aung, N.; Zhou, W. Studies on the influence of chloride ion and pH on the corrosion and electrochemical behaviour of AZ91D magnesium alloy. *J. Appl. Electrochem.* **2000**, *30*, 865–874. [CrossRef]

18. Williams, G.; Grace, R. Chloride-induced filiform corrosion of organic-coated magnesium. *Electrochim. Acta* **2011**, *56*, 1894–1903. [CrossRef]

19. Wang, Y.; Xu, W.; Wang, X.; Jiang, Q.; Li, Y.; Huang, Y.; Yang, L. Research on Dynamic Marine Atmospheric Corrosion Behavior of AZ31 Magnesium Alloy. *Metals* **2022**, *12*, 1886. [CrossRef]

20. Xin, Y.; Huo, K.; Tao, H.; Tang, G.; Chu, P.K. Influence of aggressive ions on the degradation behavior of biomedical magnesium alloy in physiological environment. *Acta Biomater.* **2008**, *4*, 2008–2015. [CrossRef]

21. Huang, C.A.; Lin, C.K.; Yeh, Y.H. Corrosion behavior of Cr/Cu-coated Mg alloy (AZ91D) in 0.1 M $H_2SO_4$ with different concentrations of NaCl. *Corrosion Sci.* **2010**, *52*, 1326–1332. [CrossRef]

22. Merachtsaki, D.; Tsardaka, E.-C.; Anastasiou, E.; Zouboulis, A. Study of Magnesium Hydroxide Protective Coating against Corrosion, Applied on Poly(methyl methacrylate) Plates, By Using the Sulfuric Acid Attack Acceleration Test. *Mater. Proc.* **2021**, *5*, 4.

23. Van Phuong, N.; Moon, S.; Chang, D.; Lee, K.H. Effect of microstructure on the zinc phosphate conversion coatings on magnesium alloy AZ91. *Appl. Surf. Sci.* **2013**, *264*, 70–78. [CrossRef]

24. Fazal, B.R.; Moon, S. Effect of Fluoride Conversion Coating on the Corrosion Resistance and Adhesion of E-painted AZ31 Magnesium Alloy. *J. Kor. Inst. Surf. Eng.* **2016**, *49*, 395–400. [CrossRef]

25. Kwon, D.; Song, P.; Moon, S. Effect of Pre-Treatment of AZ91 Mg Alloy in HF Solution on PEO Film Formation Behavior. *J. Korean Inst. Surf. Eng.* **2021**, *54*, 184–193.

26. Kwon, D.; Song, P.; Moon, S. Effect of Pre-Treatment in 0.5 M Oxalic Acid Containing Various $NH_4F$ Concentrations on PEO Film Formation of AZ91 Mg Alloy. *J. Kor. Inst. Surf. Eng.* **2022**, *55*, 24–31.

27. Kwon, D.; Pham, H.V.; Song, P.; Moon, S. Electrochemical behavior of AZ31 Mg alloy in neutral aqueous solutions containing various anions. *J. Electrochem. Sci. Technol.* accepted for publication.

28. Singh, I.B.; Singh, M.; Das, S. A comparative corrosion behavior of Mg, AZ31 and AZ91 alloys in 3.5% NaCl solution. *J. Magnes. Alloy* **2015**, *3*, 142–148. [CrossRef]

29. Atrens, A.; Shi, Z.; Mehreen, S.U.; Johnston, S.; Song, G.-L.; Chen, X.; Pan, F. Review of Mg alloy corrosion rates. *J. Magnes. Alloy* **2020**, *8*, 989–998. [CrossRef]